

Crystal Structures of Nitronium Tetranitratogallate and Its Reversible Solid-State Phase Transition Mediated by Nonmerohedral Twinning

Daniel G. Colombo, Victor G. Young, Jr.,* and Wayne L. Gladfelter*

Department of Chemistry, University of Minnesota, Minneapolis, Minnesota 55455

Received March 3, 2000

Single-crystal X-ray crystallographic analyses of $[\text{NO}_2][\text{Ga}(\text{NO}_3)_4]$ reveal that it undergoes a reversible phase transition without any apparent damage to the crystal during repeated temperature cyclings. The room-temperature, noncentrosymmetric, body-centered tetragonal ($I\bar{4}$), polymorph **1** ($a = 9.2774(3)$ Å, $c = 6.1149(2)$ Å, $Z = 2$) consists of well-separated nitronium and tetranitratogallate ions. The $[\text{Ga}(\text{NO}_3)_4]^-$ units exhibit a slightly squashed tetrahedral geometry in which all of the ligands are monodentate. Below approximately 250 K, distortions lower the symmetry to the chiral, body-centered monoclinic nonstandard space group $I2$. Both components (**2a**: $a = 9.5857(2)$ Å, $b = 5.9399(1)$ Å, $c = 8.9759(2)$ Å, $\beta = 90.409(1)^\circ$, $Z = 2$. **2b**: $a = 9.5898(2)$ Å, $b = 5.9376(1)$ Å, $c = 8.9784(1)$ Å, $\beta = 90.420(1)^\circ$, $Z = 2$) of the nonmerohedrally twinned structure are independently refined and found to be enantiomeric with nearly identical distance and angle parameters. As in the high-temperature polymorph, the cations and anions are well separated. The most notable change involves two of the nitrate ligands in the $[\text{Ga}(\text{NO}_3)_4]^-$ ions that have become bidentate, causing the molecular structure to distort toward octahedral geometry.

Introduction

The covalent nature of the bonding in anhydrous metal nitrates increases their volatility and chemical reactivity,¹ rendering these compounds attractive as carbon- and hydrogen-free single-source precursor molecules for the chemical vapor deposition (CVD) of metal oxide films.^{2–4} We recently demonstrated their use in the CVD of high- κ dielectrics in microelectronic devices.² In the course of this research, we have found that $[\text{NO}_2][\text{Ga}(\text{NO}_3)_4]$ ⁵ produces amorphous films of gallium oxide.³ The current study reports the single-crystal X-ray diffraction study of $[\text{NO}_2][\text{Ga}(\text{NO}_3)_4]$ and the observation that nitronium tetranitratogallate undergoes a reversible phase transition from a room-temperature tetragonal phase to a lower temperature nonmerohedrally twinned monoclinic phase.

Experimental Section

General Procedures. All reactions and reagent preparations, unless otherwise noted, were carried out under dry nitrogen using standard Schlenk or drybox techniques. Gallium(III) chloride (Strem) was sublimed in vacuo and stored in sealed glass ampules prior to use. Fuming nitric acid (Aldrich or Fisher, >90% HNO_3) was used as received but was stored with desiccant and out of contact with direct light to minimize decomposition. Anhydrous phosphorus pentoxide (Aldrich) was used as received. All IR spectra were recorded using a Nicolet Magna 560 FTIR spectrometer. Because of the intrinsic

reactivity of anhydrous metal nitrates toward organic substrates, all IR spectra were obtained for Fluorolube mulls using NaCl salt plates. Elemental analyses were performed by Schwartzkopf Microanalytical Laboratory (Woodside, NY).

Synthesis of Dinitrogen Pentoxide. CAUTION! Fuming nitric acid and dinitrogen pentoxide are both powerful nitrating and oxidizing agents. Contact of these compounds with any organic substrate should be avoided. All ground-glass joints should be greased with Krytox, and only Teflon stopcocks and valves should be used. Through its central neck, a flame-dried and nitrogen-purged three-neck, round-bottom 1000 mL flask was charged with 60 mL (94.44 g, 1.50 mol) of fuming nitric acid. The flask was flushed with nitrogen, after which the open neck was sealed using a glass stopper fitted with a Teflon sleeve. The HNO_3 was solidified by cooling with a liquid-nitrogen bath, and 425 g (1.50 mol) of P_4O_{10} was then quickly added to the flask, which was again flushed with nitrogen and sealed. Throughout the experiment, the entire reaction apparatus was protected from direct light. The gas supply was changed from nitrogen to oxygen, the liquid-nitrogen bath was removed, and the contents of the reaction flask were allowed to warm slowly to ambient temperature. As the flask contents were warming, a stream (5 bubbles/s) of oxygen (dried by bubbling the gas through a H_2SO_4 bubbler and a 40 cm column of Drierite and 4 Å Linde sieves) was flushed through the entire reaction apparatus into a silicone oil bubbler. The receiver flask used as a trap for N_2O_5 was cooled using a dry ice/2-propanol bath. After approximately 45 min, a large volume of reddish gas rapidly evolved from the reaction flask; this was swept by O_2 through the apparatus to condense in the trap as a white, crystalline solid. The O_2 is important both for enhancing the efficiency of mass transport of gaseous N_2O_5 to the trap and for stabilizing the N_2O_5 . After gas evolution had ceased, the reaction flask was gently warmed to 40 °C using an oil bath. Further gas evolution occurred at this temperature. After gas evolution was complete, the temperature was maintained at 40 °C for 6–8 h under the stream of O_2 . The reaction flask was then allowed to cool to ambient temperature, and all stopcocks were closed to isolate the receiver trap. The receiver flask was immediately removed and attached to another reaction apparatus setup to synthesize $[\text{NO}_2][\text{Ga}(\text{NO}_3)_4]$. Although crude N_2O_5 yields of up to 80% have been reported, no attempt to recover pure N_2O_5 was made; the crude material was used as synthesized.

- (1) Addison, C. C.; Logan, N. *Adv. Inorg. Chem. Radiochem.* **1964**, 6, 71–142.
- (2) Gilmer, D. C.; Colombo, D. G.; Taylor, C. J.; Roberts, J.; Haugstad, G.; Campbell, S. A.; Kim, H.-S.; Wilk, G. D.; Gribelyuk, M. A.; Gladfelter, W. L. *Chem. Vap. Deposition* **1998**, 4, 9–11.
- (3) Colombo, D. G.; Gilmer, D. C.; Young, V. G., Jr.; Campbell, S. A.; Gladfelter, W. L. *Chem. Vap. Deposition* **1998**, 4, 220–222.
- (4) Taylor, C. J.; Gilmer, D. C.; Colombo, D. G.; Wilk, G. D.; Campbell, S. A.; Roberts, J.; Gladfelter, W. L. *J. Am. Chem. Soc.* **1999**, 121, 5220–5229.
- (5) Bowler, D.; Logan, N. *J. Chem. Soc., Chem. Commun.* **1971**, 582–583.

Table 1. Crystallographic Data for Compounds **1**, **2a**, and **2b**^a

	1	2a/2b
empirical formula	GaN ₅ O ₁₄	GaN ₅ O ₁₄
fw	363.77	363.77
space group	<i>I</i> $\bar{4}$	<i>I</i> 2
<i>a</i> , Å	9.2774(3)	9.5857(2)/9.5898(2)
<i>b</i> , Å	9.2774(3)	5.9399(1)/5.9376(1)
<i>c</i> , Å	6.1149(2)	8.9759(2)/8.9784(1)
β , deg		90.409(1)/90.420(1)
<i>V</i> , Å ³	526.31(3)	511.06(2)/511.22(2)
<i>Z</i>	2	2
λ , Å	0.710 73	0.710 73
ρ (calcd), g cm ⁻³	2.295	2.364/2.363
μ , cm ⁻¹	27.18	27.99/27.98
<i>T</i> , K	298(2)	173(2)
<i>R</i> ₁ , w <i>R</i> ₂ [<i>I</i> > 2 σ (<i>I</i>)] ^b	0.0228, 0.0570	0.0384/0.0470, 0.0990/0.1284

^a The double values listed are for the independently refined twins **2a** and **2b**, respectively. ^b $R_1 = \sum ||F_o| - |F_c|| / \sum |F_o|$; $wR_2 = [\sum w(F_o^2 - F_c^2)^2 / \sum w(F_o^2)^2]^{1/2}$, where $w = 1/[\sigma^2(F_o^2) + (aP)^2 + bP]$, $P = (F_o^2 + 2F_c^2)/3$, and *a* and *b* are constants given in the Supporting Information.

Synthesis of [NO₂][Ga(NO₃)₄]. *Caution!* Nitronium tetranitratogallate is a nitrating agent. Precautions similar to those mentioned above should be employed. For this synthesis, modifications of published procedures^{5,6} were used. In a drybox, 5.00 g (28.8 mmol) of anhydrous GaCl₃ was placed in a flame-dried three-neck, round-bottom 250 mL reaction flask equipped with two gas adapters, a condenser, and a Teflon-coated magnetic stirbar. The reaction flask was cooled with liquid nitrogen, and the freshly prepared N₂O₅ was condensed in vacuo onto the GaCl₃. After the vacuum transfer of N₂O₅ was complete, the receiver trap was removed, a gas adapter was attached to the reaction flask on top of the condenser assembly, and a silicone oil bubbler was attached to the gas adapter. The reaction flask was allowed to warm to ambient temperature over the course of 1.5 h while direct exposure to light was avoided. The volatile byproduct ClNO₂ was allowed to vent through the bubbler. Cooling the reaction flask with an ice bath moderated the rate of gas evolution. The biphasic reaction mixture was stirred for an additional 20 h, during which the red color deepened substantially and NO₂ gas was visible in the headspace of the reaction apparatus. The N₂O₄ generated during the reaction and any residual volatiles were removed by flushing the reaction flask with dry N₂ until a crude crystalline, yellow mass remained. The solid mass was outgassed in vacuo for several hours at 15 °C. The crude material was recovered in the drybox and placed in a sublimator as a finely ground powder. The crude pale yellow product was purified by sublimation at 80 °C and 0.05 mmHg, yielding 2.91 g (8.02 mmol, 27.8% yield) of air-sensitive, translucent white crystalline blocks; the sublimed material was indefinitely stable toward decomposition while stored under N₂ or Ar. Crystals suitable for single-crystal X-ray analysis were obtained by slow sublimation over 5–7 d. FTIR: ν (N–O), nitril cation, antisymmetric, 2369 cm⁻¹ (Fluorolube mull on NaCl plates).

Crystallographic Structure Determinations of the Polymorphs of [NO₂][Ga(NO₃)₄]. Diffraction data were collected using a Siemens SMART platform CCD with specimens mounted in a Lindeman capillary (for studies at 298 K) or frozen in a Krytox film on a glass fiber (for data collection at 173 K). The 298 K phase crystallized in the tetragonal in space group *I* $\bar{4}$. All four nitrate ligands were equivalent in this noncentrosymmetric space group. The crystal data and X-ray experimental details are summarized in Table 1. Lowering the temperature below ca. 250 K caused a phase change where the crystal system was lowered to monoclinic. Possible space group choices were the conventional *C*2 and the nonstandard *I*2. The latter was chosen to facilitate direct comparisons between the phases. An additional complication in the phase change was the appearance of a nonmerohedral twin with both components present in nearly equal amounts. Dirax⁷ was used to index the twin components from a set of 50

Table 2. Atomic Fractional Coordinates for **1**, **2a**, and **2b**

atom	<i>x</i>	<i>y</i>	<i>z</i>
Complex 1			
Ga(1)	1.0000	0.5000	0.7500
O(1)	0.8286(2)	0.5378(2)	0.9062(3)
O(2)	0.7345(2)	0.6903(3)	1.1287(4)
O(3)	0.9613(3)	0.7056(3)	1.0477(4)
O(4)	0.5000	0.5000	1.1818(16)
N(1)	0.8425(2)	0.6511(2)	1.0350(3)
N(2)	0.5000	0.5000	1.0000
Complex 2a			
Ga(1)	0.0000	0.0000	0.0000
O(1)	0.1607(3)	0.1774(5)	-0.0302(3)
O(2)	0.0568(3)	0.3173(5)	-0.2288(3)
O(3)	0.2771(3)	0.3796(5)	-0.1856(3)
O(4)	0.0442(3)	-0.1292(5)	0.1918(3)
O(5)	0.1621(5)	-0.2925(6)	0.0212(4)
O(6)	0.1899(4)	-0.3938(6)	0.2552(4)
O(7)	0.5000	0.1530(12)	0.0000
O(8)	0.5000	0.5280(18)	0.0000
N(1)	0.1642(3)	0.2976(5)	-0.1559(3)
N(2)	0.1391(3)	-0.2822(5)	0.1583(4)
N(3)	0.5000	0.3387(15)	0.0000
Complex 2b			
Ga(1)	0.0000	0.0000	0.0000
O(1)	0.1606(4)	-0.1781(6)	-0.0302(4)
O(2)	0.0572(4)	-0.3177(7)	-0.2295(5)
O(3)	0.2768(4)	-0.3793(7)	-0.1861(4)
O(4)	-0.0441(4)	0.1291(7)	-0.1919(4)
O(5)	-0.1633(7)	0.2912(8)	-0.0215(5)
O(6)	-0.1901(5)	0.3942(8)	-0.2567(6)
O(7)	0.5000	0.8474(15)	0.0000
O(8)	0.5000	0.4711(20)	0.0000
N(1)	0.1640(4)	-0.2971(7)	-0.1558(4)
N(2)	-0.1393(4)	-0.2823(7)	-0.1581(5)
N(3)	0.5000	0.6605(19)	0.0000

randomly selected reflections, and Gemini⁸ was used to determine the putative twin laws. Both twin components were integrated using SAINT.⁹ The cell constants of the components were derived using 4038 and 4002 reflections, respectively, from the separate integrations. Absorption corrections were applied by using SADABS.¹⁰ The structures of both twin components were independently solved by direct methods, and refinements indicated that they were enantiomeric twins. UNTWIN¹¹ was used to correct the data for partially and exactly overlapped reflections between the twin components; approximately one-third of the data required correction. The crystal data and details of the intensity collection and refinement procedures for both twin components are also included in Table 1. Refinements uncorrected for twinning produced *R*_i residuals of 0.0735 and 0.0942, but with corrections, these improved to 0.0384 and 0.0470, respectively. All reflections were retained throughout the refinements. No refinement was attempted with data excluding the overlapping reflections. Both twin components (**2a** and **2b**) are believed to have the correct handedness on the basis of the Flack absolute structure parameter. The atomic coordinates for **1**, **2a**, and **2b** are listed in Table 2, and complete crystallographic details are provided in the Supporting Information.

Results and Discussion

Excess dinitrogen pentoxide and gallium(III) chloride, onto which it was condensed in vacuo at -198 °C, reacted to yield

(8) *Software for Indexing and Correcting Data Affected by Non-merohedral Twinning*; Bruker-AXS, Inc.: Madison, WI, 1999.

(9) *Area Detector Integration Software*, Version 4.05; Bruker-AXS, Inc.: Madison, WI, 1995.

(10) Blessing, R. H. *Acta Crystallogr.* **1995**, *A51*, 33.

(11) Young, V. G., Jr. University of Minnesota. Unpublished work, 1997. The metric tensor, the twin law, and an algorithm for partially overlapped reflections were used to output a corrected HKLF 5 SHELX reflection file. Partially overlapped reflections were grouped in separate batches in ascending 0.005 Å⁻¹ sets in the range 0.00–0.025 Å⁻¹.

(6) Ivanov-Emin, B. N.; Odinets, Z. K.; Yushchenko, S. F.; Zaitsev, B. E.; Ezhov, A. I. *Russ. J. Inorg. Chem. (Engl. Transl.)* **1975**, *20*, 843–846.

(7) Duisenberg, A. J. M. *J. Appl. Crystallogr.* **1992**, *25*, 92.

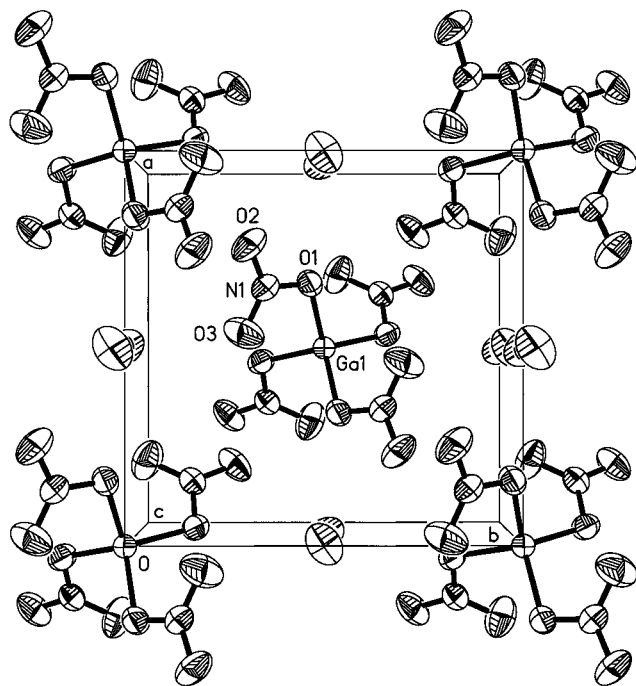


Figure 1. Thermal ellipsoid drawing of the crystal structure of polymorph **1** at the 50% probability level.

Table 3. Selected Bond Lengths (Å) and Angles (deg) for Polymorph **1** of $[\text{NO}_2][\text{Ga}(\text{NO}_3)_4]$

Ga(1)–O(1)	1.888(2)	N(1)–O(1)	1.320(3)
N(1)–O(2)	1.210(3)	N(1)–O(3)	1.214(3)
N(2)–O(4)	1.112(9)		
O(1)–Ga(1)–O(1A)	104.84(6)	O(1)–Ga(1)–O(1B)	119.21(13)
N(1)–O(1)–Ga(1)	115.59(14)	O(2)–N(1)–O(3)	126.6(3)
O(2)–N(1)–O(1)	116.2(2)	O(3)–N(1)–O(1)	117.2(2)
O(4)–N(2)–O(4A)	180		

$[\text{NO}_2][\text{Ga}(\text{NO}_3)_4]$ during gradual warming to 25 °C. A crude white solid was recovered after the removal of all volatiles at 15 °C and 0.05 Torr. Slow vacuum sublimation of the crude white solid resulted in the formation of air-sensitive, translucent white crystalline plates; the sublimed material was stable toward decomposition while stored under N_2 or Ar. The IR spectrum of the sublimed material in a fluorolube mull had a discernible band of moderate intensity at 2369 cm^{-1} that was assigned to the nitronium ion.

Single-crystal structural analyses revealed that $[\text{NO}_2][\text{Ga}(\text{NO}_3)_4]$ underwent a reversible phase transition with no apparent damage to the crystal. The room-temperature polymorph **1** (Figure 1 and Table 3) was indexed to a tetragonal cell in the noncentrosymmetric space group $I\bar{4}$. The low-temperature nonmerohedrally twinned monoclinic phase **2a/2b** (Figure 2 and Table 4) was indexed in the nonstandard space group $I2$. The phase transition was estimated to occur near 250 K. Comparison of the a lattice constants of **2a/2b** with a of **1** shows an increase of 0.31 Å. This increase is matched by a corresponding decrease (0.30 Å) in c of **2a/2b** relative to a of **1**. The twin components in **2a/2b** were present in a 1:1 ratio. The difference in unit cell volumes at the two different temperatures would seem reasonable even if no phase transition occurred. In the report by Ivanov-Emin et al. describing the reaction of gallium halides with N_2O_5 , the formula of the sublimed white crystalline compound was $\text{Ga}(\text{NO}_3)_3$.⁶ Comparison of the experimental powder diffraction pattern with that calculated for **1** establishes that they are not the same compound. The formula and structure

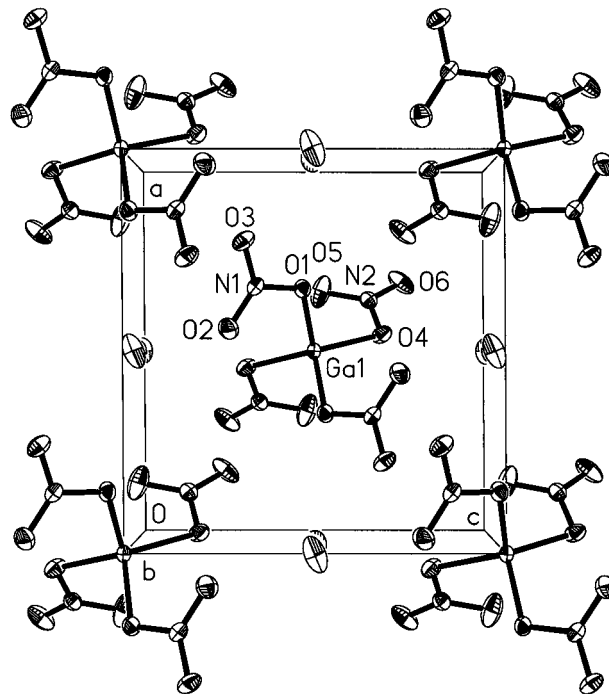


Figure 2. Thermal ellipsoid drawing of the crystal structure of polymorph **2a** at the 50% probability level.

of **1** are consistent with the compound synthesized by Bowler and Logan.⁵

The four, equivalent, nitrates in **1** are monodentate. The Ga(1)–O(1) bond distance is 1.888(2) Å, while the next nearest Ga–O interaction, Ga(1)–O(3), is 2.657(3) Å. The geometry of the complex ion can best be described as a tetrahedron that is slightly squashed along the $\bar{4}$ axis. A simple measure of this distortion can be obtained by comparing the O(1)–Ga(1)–O(1B) angle, where the nitrates are related by a 2-fold rotation, to the angle for the $\bar{4}$ relationship between the nitrates expressed as O(1)–Ga(1)–O(1A). These values are 119.21(3) and 104.84(6)°, respectively. At 1.320(3) Å, the N(1)–O(1) bond is longer than both N(1)–O(2) and N(1)–O(3) (1.210(3) and 1.214(3) Å, respectively). Although the nitrate ligand remains planar, these distortions in bond lengths accompany an enlargement of the O(2)–N(1)–O(3) angle relative to the other O–N–O angles.

The bond distances in the independently refined twins of the low-temperature polymorph, **2a/2b**, are equivalent within two standard deviations; therefore, only one set of the numbers (from **2a**) will be quoted in this discussion (both sets appear in Table 4). The important change in the geometry involves the motion of two of the nitrate ligands to allow a weak, bidentate interaction. The lowered symmetry gives rise to three independent Ga–O bond distances. The two equivalent monodentate nitrates (Ga(1)–O(1)) exhibit the shortest bonds at 1.887(3) Å, indistinguishable from those found for the monodentate nitrates in **1**. At 1.929(3) Å, the stronger interactions of the bidentate ligands are significantly longer than the monodentate Ga–O distances. Finally, the weaker interactions of the bidentate ligands, Ga(1)–O(5), are 2.338(4) Å. The existence of asymmetric bidentate nitrates has been demonstrated for several transition and main group metal complexes.¹²

As the motion toward chelation progresses, the changes in the O–Ga–O angles are characteristic of a change from a four-

(12) Sisler, H. H. In *Encyclopedia of Inorganic Chemistry*; King, R. B., Ed.; Wiley: New York, 1994; Vol. 5, p 2544.

Table 4. Selected Bond Lengths (Å) and Angles (deg) for the Low-Temperature Polymorph of $[\text{NO}_2][\text{Ga}(\text{NO}_3)_4]^a$

Ga(1)–O(1)	1.887(3)/1.889(3)	O(1)–N(1)	1.336(4)/1.331(5)	O(6)–N(2)	1.195(5)/1.207(6)	N(2)–O(4)	1.332(4)/1.325(5)
Ga(1)–O(4)	1.929(3)/1.929(4)	O(2)–N(1)	1.222(4)/1.221(6)	N(2)–O(5)	1.253(5)/1.251(6)	N(3)–O(7)	1.10(1)/1.11(1)
Ga(1)–O(5)	2.338(4)/2.340(6)	O(3)–N(1)	1.218(4)/1.220(6)	N(3)–O(8)	1.12(1)/1.12(2)		
O(1)–Ga(1)–O(1A)	112.1(2)/111.9(2)	O(1)–Ga(1)–O(4)	101.1(1)/105.5(2)				
O(1A)–Ga(1)–O(4)	105.6(1)/100.2(2)	O(4)–Ga(1)–O(4A)	133.1(2)/133.2(3)				
O(4)–Ga(1)–O(5A)	85.3(1)/85.5(2)	O(1)–Ga(1)–O(5A)	161.1(1)/83.1(2)				
O(4)–Ga(1)–O(5)	59.3(1)/59.4(2)	O(1)–Ga(1)–O(5)	83.3(1)/161.4(2)				
O(5A)–Ga(1)–O(5)	84.0(2)/84.7(3)	N(1)–O(1)–Ga(1)	116.4(2)/116.4(3)				
O(3)–N(1)–O(2)	126.3(3)/125.5(4)	O(3)–N(1)–O(1)	115.2(3)/115.4(4)				
O(2)–N(1)–O(1)	118.5(3)/119.1(4)	O(6)–N(2)–O(5)	127.9(4)/128.3(5)				
O(6)–N(2)–O(4)	119.6(3)/119.0(5)	O(5)–N(2)–O(4)	112.5(4)/112.7(4)				
N(2)–O(4)–Ga(1)	102.6(2)/102.4(3)	N(2)–O(5)–Ga(1)	85.5(3)/85.5(3)				
O(7)–N(3)–O(8)	180/180						

^a The double values listed are for the independently refined twins **2a** and **2b**, respectively.

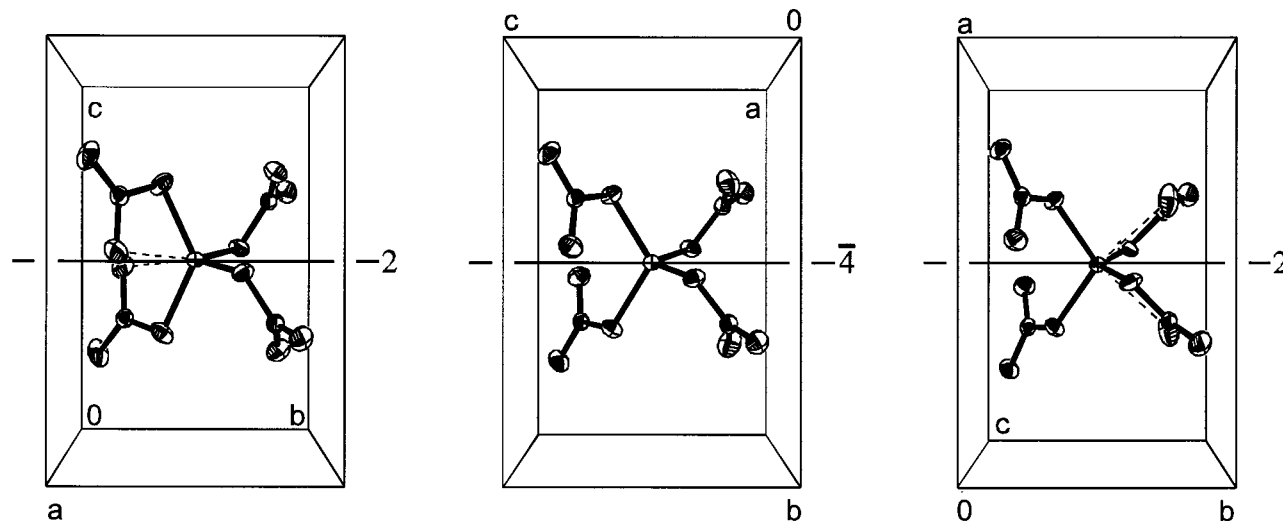


Figure 3. Relationship among the structures of the high-temperature tetragonal polymorph (central figure) and the two enantiomeric twins of the low-temperature polymorph. The orientations of the cells are arranged to emphasize the similarities among the three structures. The scales of the drawings are identical, and the thermal ellipsoids of the high- and low-temperature polymorphs are shown at 20% and 50% probability levels, respectively.

coordinate, tetrahedral geometry to an octahedral structure. One of the two equivalent O–Ga–O angles bisected by the *c* axis in **1** (O(1)–Ga(1)–O(1B)) closes from 119.21(13) to 112.1(2)° for O(1)–Ga(1)–O(1A) in **2a/2b**. The equivalent angle on the opposite side of the gallium in **1** opens to 133.1(2)° in **2a/2b**. Relatively smaller changes occur in the remaining O–Ga–O angles.

The nitrate ligands also reflect the additional interactions with the gallium, although the changes are small. In **2a/2b**, each monodentate nitrate exhibits parameters similar to those found in **1**. Each bidentate nitrate shows a shortening of N(2)–O(6) to 1.195(5) Å and a lengthening of N(2)–O(5) to 1.253(5) Å. Each O(4)–N(2)–O(5) angle, which is part of a developing ring incorporating the gallium, is decreased to 112.5(4)°.

The nitronium ions occupy special positions in both polymorphs, extending along channels parallel to the crystallographic *c* axis for **1** and along channels parallel to the crystallographic *b* axis for **2a/2b**. There are no unusually close contacts with the tetranitratogallate anion in either polymorph. The relative positions of the $[\text{NO}_2]^+$ and $[\text{Ga}(\text{NO}_3)_4]^-$ ions change only slightly during the phase transition. The four symmetry-related Ga(1)–N(2) nearest-neighbor distances of 4.884 Å in **1** change to two distances each of 4.589 and 5.198 Å (note that the average is 4.894 Å). Considering the relatively open channels along which the nitronium ions are located in **1**, it is not surprising to find that N(2) and O(4) exhibit relatively large anisotropic displacements parallel to the *c* axis.

Figure 3 focuses on the changes in the $[\text{Ga}(\text{NO}_3)_4]^-$ ion during the phase transition. The central drawing shows the high-temperature, tetragonal, polymorph. As the temperature is lowered, the formation of the weak Ga–O interactions drives the phase transition to the lower symmetry structures located on either side in Figure 3. There is an equal probability for this to occur along $[001]$ or $[00\bar{1}]$ in **1**. Due to the polar nature of the low-temperature structure (*I2* space group), as soon as the contents of one unit cell change, a local dipole moment is formed. Considering the cooperative nature of these interactions, this initial dipole may influence neighboring unit cells, leading to one of the twin domains. Although we have no information that reveals the sizes of the twin domains, from the lack of broadening seen in the X-ray diffraction reflections, they must each be at least 20 nm in diameter. What is perhaps most surprising is that the phase transition is reversible without noticeable destruction of a single crystal. This would be less unusual in the absence of twinning.

Acknowledgment. This research was supported by a grant from the National Science Foundation (CHE-9616501).

Supporting Information Available: X-ray crystallographic files, in CIF format, for the structure determinations of **1** and both twins of **2a/2b**. This material is available free of charge via the Internet at <http://pubs.acs.org>.